Conditional Adversarial Domain Adaptation

Mingsheng Long[†], **Zhangjie Cao**[†], **Jianmin Wang**[†], **and Michael I. Jordan**[♯]
[†]School of Software, Tsinghua University, China
[†]KLiss, MOE; BNRist; Research Center for Big Data, Tsinghua University, China
[♯]University of California, Berkeley, Berkeley, USA
{mingsheng,jimwang}@tsinghua.edu.cn caozhangjie14@gmail.com
jordan@berkeley.edu

Abstract

Adversarial learning has been embedded into deep networks to learn disentangled and transferable representations for domain adaptation. Existing adversarial domain adaptation methods may struggle to align different domains of multimodal distributions that are native in classification problems. In this paper, we present conditional adversarial domain adaptation, a principled framework that conditions the adversarial adaptation models on discriminative information conveyed in the classifier predictions. Conditional domain adversarial networks (CDANs) are designed with two novel conditioning strategies: multilinear conditioning that captures the cross-covariance between feature representations and classifier predictions to improve the discriminability, and entropy conditioning that controls the uncertainty of classifier predictions to guarantee the transferability. Experiments testify that the proposed approach exceeds the state-of-the-art results on five benchmark datasets.

1 Introduction

Deep networks have significantly improved the state-of-the-arts for diverse machine learning problems and applications. When trained on large-scale datasets, deep networks learn representations which are generically useful across a variety of tasks [36, 11, 55]. However, deep networks can be weak at generalizing learned knowledge to new datasets or environments. Even a subtle change from the training domain can cause deep networks to make spurious predictions on the target domain [55, 52]. While in many real applications, there is the need to transfer a deep network from a source domain where sufficient training data is available to a target domain where only unlabeled data is available, such a transfer learning paradigm is hindered by the shift in data distributions across domains [39].

Learning a model that reduces the dataset shift between training and testing distributions is known as domain adaptation [38]. Previous domain adaptation methods in the shallow regime either bridge the source and target by learning invariant feature representations or estimating instance importances using labeled source data and unlabeled target data [24, 37, 15]. Recent advances of deep domain adaptation methods leverage deep networks to learn transferable representations by embedding adaptation modules in deep architectures, simultaneously disentangling the explanatory factors of variations behind data and matching feature distributions across domains [12, 13, 29, 53, 31, 30, 51].

Adversarial domain adaptation [12, 53, 51] integrates adversarial learning and domain adaptation in a two-player game similarly to Generative Adversarial Networks (GANs) [17]. A domain discriminator is learned by minimizing the classification error of distinguishing the source from the target domains, while a deep classification model learns transferable representations that are indistinguishable by the domain discriminator. On par with these feature-level approaches, generative pixel-level adaptation models perform distribution alignment in raw pixel space, by translating source data to the style of a target domain using Image to Image translation techniques [57, 28, 22, 43]. Another line of works align distributions of features and classes separately using different domain discriminators [23, 8, 50].

32nd Conference on Neural Information Processing Systems (NIPS 2018), Montréal, Canada.

Despite their general efficacy for various tasks ranging from classification [12, 51, 28] to segmentation [43, 50, 22], these adversarial domain adaptation methods may still be constrained by two bottlenecks. First, when data distributions embody complex multimodal structures, adversarial adaptation methods may fail to capture such multimodal structures for a discriminative distribution alignment without mode mismatch. Such a risk comes from the equilibrium challenge of adversarial learning in that even if the discriminator is fully confused, we have no guarantee that two distributions are sufficiently similar [3, 4]. Note that this risk cannot be tackled by aligning distributions of features and classes via separate domain discriminators as [23, 8, 50], since the multimodal structures can only be captured sufficiently by the cross-covariance dependency between the features and classes [47, 44]. Second, it is risky to condition the domain discriminator on the discriminative information when it is uncertain.

In this paper, we tackle the two aforementioned challenges by formalizing a conditional adversarial domain adaptation framework. Recent advances in the Conditional Generative Adversarial Networks (CGANs) [34, 35] disclose that the distributions of real and generated images can be made similar by conditioning the generator and discriminator on discriminative information. Motivated by the conditioning insight, this paper presents Conditional Domain Adversarial Networks (CDANs) to exploit discriminative information conveyed in the classifier predictions to assist adversarial adaptation. The key to the CDAN models is a novel conditional domain discriminator conditioned on the cross-covariance of domain-specific feature representations and classifier predictions. We further condition the domain discriminator on the uncertainty of classifier predictions, prioritizing the discriminator on easy-to-transfer examples. The overall system can be solved in linear-time through back-propagation. Based on the domain adaptation theory [5], we give a theoretical guarantee on the generalization error bound. Experiments show that our models exceed state-of-the-art results on five benchmark datasets.

2 Related Work

Domain adaptation [38, 39] generalizes a learner across different domains of different distributions, by either matching the marginal distributions [49, 37, 15] or the conditional distributions [56, 10]. It finds wide applications in computer vision [42, 18, 16, 21] and natural language processing [9, 14]. Besides the aforementioned shallow architectures, recent studies reveal that deep networks learn more transferable representations that disentangle the explanatory factors of variations behind data [6] and manifest invariant factors underlying different populations [14, 36]. As deep representations can only reduce, but not remove, the cross-domain distribution discrepancy [55], recent research on deep domain adaptation further embeds adaptation modules in deep networks using two main technologies for distribution matching: moment matching [52, 29, 31, 30] and adversarial training [12, 53, 13, 51].

Pioneered by the Generative Adversarial Networks (GANs) [17], the adversarial learning has been successfully explored for generative modeling. GANs constitute two networks in a two-player game: a generator that captures data distribution and a discriminator that distinguishes between generated samples and real data. The networks are trained in a minimax fashion such that the generator is learned to fool the discriminator while the discriminator struggles to be not fooled. Several difficulties of GANs have been addressed, e.g. improved training [2, 1] and mode collapse [34, 7, 35], but others still remain, e.g. failure in matching distributions [4, 3]. Towards adversarial learning for domain adaptation, unconditional ones have been leveraged while conditional ones remain under explored.

Sharing some spirit of conditional GANs [3, 4], another line of works model the features and classes using separate domain discriminators. Hoffman *et al.* [23] performs global domain alignment by learning features to deceive the domain discriminator, and category specific adaptation by minimizing a constrained multiple instance loss. In particular, the adversarial module for feature representation is not conditioned on the class-adaptation module for class information. Chen *et al.* [8] performs class-wise alignment over the classifier layer; i.e., multiple domain discriminators take as inputs only the softmax probabilities of source classifier, rather than conditioned on the class information. Tsai *et al.* [50] imposes two independent domain discriminators on the feature and class layers. These methods do not explore the dependency between the features and classes in a unified conditional domain discriminator, which is important to capture the multimodal structures underlying data distributions.

This paper extends the conditioning adversarial mechanism to enable discriminative and transferable domain adaptation, by defining the domain discriminator on the features while conditioning it on the class information. Two novel conditioning strategies are designed to capture the cross-covariance dependency between the feature representations and class predictions while controlling the uncertainty of classifier predictions. This is different from aligning the features and classes separately [23, 8, 50].

3 Conditional Adversarial Domain Adaptation

In unsupervised domain adaptation, we are given a source domain $\mathcal{D}_s = \{(\mathbf{x}_i^s, \mathbf{y}_i^s)\}_{i=1}^{n_s}$ of n_s labeled examples and a target domain $\mathcal{D}_t = \{\mathbf{x}_j^t\}_{j=1}^{n_t}$ of n_t unlabeled examples. The source domain and target domain are sampled from joint distributions $P(\mathbf{x}^s, \mathbf{y}^s)$ and $Q(\mathbf{x}^t, \mathbf{y}^t)$ respectively, while the IID assumption is violated as $P \neq Q$. The goal of this paper is to design a deep network $\mathbf{y} = G(\mathbf{x})$ which formally reduces the shifts in the joint distributions across domains, such that the target risk $\epsilon_t(G) = \mathbb{E}_{(\mathbf{x}^t, \mathbf{y}^t) \sim Q}\left[G(\mathbf{x}^t) \neq \mathbf{y}^t\right]$ can be bounded by the source risk $\epsilon_s(G) = \mathbb{E}_{(\mathbf{x}^s, \mathbf{y}^s) \sim P}\left[G(\mathbf{x}^s) \neq \mathbf{y}^s\right]$ plus the distribution discrepancy $D(P, Q)$ embodied by a novel conditional adversarial discriminator.

Adversarial learning, the key idea to enabling Generative Adversarial Networks (GANs) [17], has been successfully explored to minimize the cross-domain discrepancy [13, 51]. Denote by $\mathbf{f} = F(\mathbf{x})$ the feature representation and by $\mathbf{g} = G(\mathbf{x})$ the classifier prediction generated from the deep network G. Domain adversarial neural network (DANN) [13] is a two-player game: the first player is the domain discriminator D trained to distinguish the source domain from the target domain and the second player is the feature representation F trained simultaneously to confuse the domain discriminator D. The error function of the domain discriminator corresponds well to the discrepancy between feature distributions $P(\mathbf{f})$ and $Q(\mathbf{f})$ [12], a key to bound the target risk in the domain adaptation theory [5].

Conditional Discriminator We further improve existing adversarial domain adaptation methods [12, 53, 51] in two directions. First, when the joint distributions of feature and class, i.e. $P(\mathbf{x}^s, \mathbf{y}^s)$ and $Q(\mathbf{x}^t, \mathbf{y}^t)$, are non-identical across domains, adapting only the feature representation $\mathbf{f}$ may be insufficient. Due to a quantitative study [55], deep representations eventually transition from general to specific along deep networks, with transferability decreased remarkably in the domain-specific feature layer $\mathbf{f}$ and classifier layer $\mathbf{g}$. In other words, the joint distributions of feature representation $\mathbf{f}$ and classifier prediction $\mathbf{g}$ should still be non-identical in these domain adversarial networks. Second, when the feature distribution is multimodal, which is a real scenario due to the nature of multi-class classification, adapting only the feature representation may be challenging for adversarial networks. Recent work [17, 2, 7, 1] reveals the high risk of failure in matching a only fraction of components underlying different distributions with adversarial networks. Namely, even if the discriminator is fully confused, we have no theoretical guarantee that two different distributions are made identical [3, 4].

This paper tackles the two aforementioned challenges by formalizing a conditional adversarial domain adaptation framework. Recent advances in Conditional Generative Adversarial Networks (CGANs) [34] disclose that different distributions can be matched better by conditioning the generator and discriminator on relevant information, such as associated labels and affiliated modality. Conditional GANs [25, 35] generate globally coherent images from datasets with high variability and multimodal distributions. Motivated by conditional GANs, we observe that in adversarial domain adaptation, the classifier prediction $\mathbf{g}$ conveys discriminative information potentially revealing the multimodal structures, which can be conditioned on when adapting feature representation $\mathbf{f}$. By conditioning, domain variances in both feature representation $\mathbf{f}$ and classifier prediction $\mathbf{g}$ can be modeled simultaneously.

We formulate Conditional Domain Adversarial Network (CDAN) as a minimax optimization problem with two competitive error terms: (a) E_G on the source classifier $\mathbf{g} = G(\mathbf{x})$, which is minimized to guarantee lower source risk; (b) $E_{D,G}$ on the source classifier $\mathbf{g} = G(\mathbf{x})$ and the domain discriminator D over the source and target domains, which is minimized over D but maximized over both F and G:

$$E_G = \frac{1}{n_s} \sum_{i=1}^{n_s} L\left(G\left(\mathbf{x}_i^s\right), \mathbf{y}_i^s\right), \tag{1}$$

$$E_{D,G} = -\frac{1}{n_s} \sum_{i=1}^{n_s} \log\left[D\left(\mathbf{f}_i^s, \mathbf{g}_i^s\right)\right] - \frac{1}{n_t} \sum_{j=1}^{n_t} \log\left[1 - D\left(\mathbf{f}_j^t, \mathbf{g}_j^t\right)\right], \tag{2}$$

where $L(\cdot, \cdot)$ is the cross-entropy loss, and $\mathbf{h} = (\mathbf{f}, \mathbf{g})$ is the joint variable of feature representation $\mathbf{f}$ and classifier prediction $\mathbf{g}$. The minimax game of conditional domain adversarial network (CDAN) is

$$\begin{aligned} &\min_G E_G - \lambda E_{D,G} \\ &\min_D E_{D,G} \end{aligned} \tag{3}$$

where λ is a hyper-parameter between the two objectives to tradeoff source risk and domain adversary.

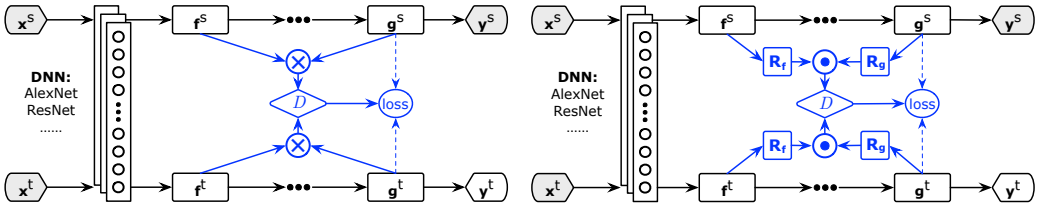

(a) Multilinear conditioning (CDAN-M) (b) Randomized Multilinear conditioning (CDAN-RM)

Figure 1: Architectures of Conditional Domain Adversarial Networks (CDAN) for domain adaptation, where domain-specific feature representation $\mathbf{f}$ and classifier prediction $\mathbf{g}$ embody the cross-domain gap and should be adapted jointly by the conditional domain discriminator D, and the entropy conditioning (dashed) is to prioritize D on easy-to-transfer examples. (a) Multilinear (M) conditioning, applicable to lower-dimensional scenario, where D is conditioned on classifier prediction $\mathbf{g}$ via multilinear map $\mathbf{f} \otimes \mathbf{g}$; (b) Randomized Multilinear (RM) conditioning, fit to higher-dimensional scenario, where D is conditioned on classifier prediction $\mathbf{g}$ via randomized multilinear map $\frac{1}{\sqrt{d}}(\mathbf{R_f f}) \odot (\mathbf{R_g g})$.

We condition domain discriminator D on the classifier prediction $\mathbf{g}$ through joint variable $\mathbf{h} = (\mathbf{f}, \mathbf{g})$. This conditional domain discriminator can potentially tackle the two aforementioned challenges of adversarial domain adaptation. A simple conditioning of D is $D(\mathbf{f} \oplus \mathbf{g})$, where we concatenate the feature representation and classifier prediction in vector $\mathbf{f} \oplus \mathbf{g}$ and feed it to conditional domain discriminator D. This conditioning strategy is widely adopted by existing conditional GANs [34, 25, 35]. However, with the concatenation strategy, $\mathbf{f}$ and $\mathbf{g}$ are independent on each other, thus failing to fully capture multiplicative interactions between feature representation and classifier prediction, which are crucial to domain adaptation. As a result, the multimodal information conveyed in classifier prediction cannot be fully exploited to match the multimodal distributions of complex domains [47].

Multilinear Conditioning Multilinear map models the multiplicative interactions between different variables. The multilinear map of infinite-dimensional nonlinear feature maps has been successfully applied to embed joint distribution or conditional distribution into reproducing kernel Hilbert spaces [47, 44, 45, 30]. Given two random vectors $\mathbf{x}$ and $\mathbf{y}$, the joint distribution $P(\mathbf{x}, \mathbf{y})$ can be modeled by the cross-covariance $\mathbb{E}_{\mathbf{xy}}[\phi(\mathbf{x}) \otimes \phi(\mathbf{y})]$, where ϕ is a feature map induced by some reproducing kernel. Such kernel embeddings enable easy manipulation of joint distributions, with the ability of modeling the cross-covariance, i.e. the multiplicative interactions across multiple random variables.

Besides the theoretical benefit of the multilinear map $\mathbf{x} \otimes \mathbf{y}$ over the concatenation $\mathbf{x} \oplus \mathbf{y}$ [47, 46], we further explain its superiority intuitively. Assume linear map $\phi(\mathbf{x}) = \mathbf{x}$ and one-hot label vector $\mathbf{y}$ in C classes. As can be verified, mean map $\mathbb{E}_{\mathbf{xy}}[\mathbf{x} \oplus \mathbf{y}] = \mathbb{E}_{\mathbf{x}}[\mathbf{x}] \oplus \mathbb{E}_{\mathbf{y}}[\mathbf{y}]$ computes the means of $\mathbf{x}$ and $\mathbf{y}$ independently. In contrast, mean map $\mathbb{E}_{\mathbf{xy}}[\mathbf{x} \otimes \mathbf{y}] = \mathbb{E}_{\mathbf{x}}[\mathbf{x}|y=1] \oplus \ldots \oplus \mathbb{E}_{\mathbf{x}}[\mathbf{x}|y=C]$ computes the means of each of the C class-conditional distributions $P(\mathbf{x}|y)$. Superior than concatenation, the multilinear map $\mathbf{x} \otimes \mathbf{y}$ can fully capture the multimodal structures behind complex data distributions.

Taking the advantage of multilinear map, in this paper, we condition D on $\mathbf{g}$ with the multilinear map

$$T_{\otimes}(\mathbf{f}, \mathbf{g}) = \mathbf{f} \otimes \mathbf{g}, \tag{4}$$

where $T_{\otimes}$ is a multilinear map and $D(\mathbf{f}, \mathbf{g}) = D(\mathbf{f} \otimes \mathbf{g})$. As such, the conditional domain discriminator successfully models the multimodal information and joint distributions of $\mathbf{f}$ and $\mathbf{g}$. Also, the multi-linearity can accommodate random vectors $\mathbf{f}$ and $\mathbf{g}$ with different cardinalities and magnitudes.

A disadvantage of the multilinear map is dimension explosion. Denoting by d_f and d_g the dimensions of vectors $\mathbf{f}$ and $\mathbf{g}$ respectively, the dimension of multilinear map $\mathbf{f} \otimes \mathbf{g}$ is $d_f \times d_g$, often too high-dimensional to be embedded into deep networks without causing parameter explosion. This paper addresses the dimension explosion by randomized methods [40, 26]. Note that multilinear map holds

$$\begin{aligned} \langle T_{\otimes}(\mathbf{f}, \mathbf{g}), T_{\otimes}(\mathbf{f}', \mathbf{g}') \rangle &= \langle \mathbf{f} \otimes \mathbf{g}, \mathbf{f}' \otimes \mathbf{g}' \rangle \\ &= \langle \mathbf{f}, \mathbf{f}' \rangle \langle \mathbf{g}, \mathbf{g}' \rangle \\ &\approx \langle T_{\odot}(\mathbf{f}, \mathbf{g}), T_{\odot}(\mathbf{f}', \mathbf{g}') \rangle, \end{aligned} \tag{5}$$

where $T_{\odot}(\mathbf{f}, \mathbf{g})$ is the explicit randomized multilinear map of dimension $d \ll d_f \times d_g$ and we define

$$T_{\odot}(\mathbf{f}, \mathbf{g}) = \frac{1}{\sqrt{d}} (\mathbf{R_f f}) \odot (\mathbf{R_g g}), \tag{6}$$

where $\odot$ is element-wise product, $\mathbf{R_f}$ and $\mathbf{R_g}$ are random matrices sampled only once and fixed in training, and each element R_{ij} follows a symmetric distribution with univariance, i.e. $\mathbb{E}\left[R_{ij}\right] = 0, \mathbb{E}[R_{ij}^2] = 1$. Applicable distributions include Gaussian distribution and Uniform distribution. As the inner-product on $T_{\otimes}$ can be accurately approximated by the inner-product on $T_{\odot}$, we can directly adopt $T_{\odot}(\mathbf{f}, \mathbf{g})$ for computation efficiency. We guarantee such approximation quality by a theorem.

Theorem 1. *The expectation and variance of randomized map $T_{\odot}\left(\mathbf{f}, \mathbf{g}\right)$ (6) for $T_{\otimes}\left(\mathbf{f}, \mathbf{g}\right)$ (4) satisfy*

$$\mathbb{E}\left[\left\langle T_{\odot}\left(\mathbf{f}, \mathbf{g}\right), T_{\odot}\left(\mathbf{f}', \mathbf{g}'\right)\right\rangle\right] = \left\langle \mathbf{f}, \mathbf{f}'\right\rangle \left\langle \mathbf{g}, \mathbf{g}'\right\rangle, \tag{7}$$

$$\operatorname{var}\left[\left\langle T_{\odot}\left(\mathbf{f}, \mathbf{g}\right), T_{\odot}\left(\mathbf{f}', \mathbf{g}'\right)\right\rangle\right] = \sum_{i=1}^{d} \beta\left(\mathbf{R}_i^{\mathbf{f}}, \mathbf{f}\right) \beta\left(\mathbf{R}_i^{\mathbf{g}}, \mathbf{g}\right) + C, \tag{8}$$

where $\beta\left(\mathbf{R}_i^{\mathbf{f}}, \mathbf{f}\right) = \frac{1}{d}\sum_{j=1}^{d_f}\left[f_j^2 {f'_j}^2 \mathbb{E}[(R_{ij}^f)^4] + C'\right]$ and similarly for $\beta\left(\mathbf{R}_i^{\mathbf{g}}, \mathbf{g}\right)$, C, C' are constants.

Proof. The proof is given in the supplemental material. □

Theorem 1 verifies that $T_{\odot}$ is an unbiased estimate of $T_{\otimes}$, with estimation variance depending only on the fourth-order moments $\mathbb{E}[(R_{ij}^f)^4]$ and $\mathbb{E}[(R_{ij}^g)^4]$, which are constants for many symmetric distributions with univariance, including Gaussian distribution and (centered) Uniform distribution. The bound reveals that we can further minimize the approximation error by normalizing the features.

For simplicity, we define the conditioning strategy used by the conditional domain discriminator D as

$$T\left(\mathbf{h}\right) = \begin{cases} T_{\otimes}\left(\mathbf{f}, \mathbf{g}\right) & \text{if } d_f \times d_g \leqslant 4096 \\ T_{\odot}\left(\mathbf{f}, \mathbf{g}\right) & \text{otherwise,} \end{cases} \tag{9}$$

where 4096 is the largest number of units in typical deep networks (e.g. AlexNet), and if dimension of the multilinear map $T_{\otimes}$ is larger than 4096, then we will opt to randomized multilinear map $T_{\odot}$.

Entropy Conditioning The minimax problem (3) for conditional domain discriminator (2) may be problematic, since the domain discriminator imposes equal importance for different examples, while hard-to-transfer examples with uncertain predictions may deteriorate the adversarial adaptation procedure. Towards safe transfer, we quantify the uncertainty of classifier predictions by the entropy criterion $H\left(\mathbf{g}\right) = -\sum_{c=1}^{C} g_c \log g_c$, where C is the number of classes and g_c is the probability of predicting an example to class c. The certainty of predictions can be computed by $e^{-H(\mathbf{g})} \in [\frac{1}{C}, 1]$. We condition the domain discriminator on the entropy-based certainty measure, which prioritizes the discriminator on those easy-to-transfer examples with certain predictions. The final discriminator with both multilinear conditioning for discriminability and entropy conditioning for transferability is

$$E_{D,G} = -\frac{1}{n_s}\sum_{i=1}^{n_s} e^{-H(\mathbf{g}_i^s)} \log\left[D\left(T\left(\mathbf{h}_i^s\right)\right)\right] - \frac{1}{n_t}\sum_{j=1}^{n_t} e^{-H\left(\mathbf{g}_j^t\right)} \log\left[1 - D\left(T\left(\mathbf{h}_j^t\right)\right)\right]. \tag{10}$$

The discriminator encourages certain predictions, satisfying the entropy minimization principle [19].

Conditional Domain Adversarial Network We enable conditional adversarial domain adaptation over the domain-specific feature representation $\mathbf{f}$ and classifier prediction $\mathbf{g}$. We jointly minimize error (1) with respect to the source classifier G, minimize error (10) with respect to domain discriminator D, and maximize error (10) with respect to the feature extractor F and the source classifier G. This leads to the minimax problem for the proposed Conditional Domain Adversarial Networks (CDANs):

$$\begin{aligned} \min_{G}\ & \frac{1}{n_s}\sum_{i=1}^{n_s} L\left(G\left(\mathbf{x}_i^s\right), \mathbf{y}_i^s\right) \\ & + \frac{\lambda}{n_s}\sum_{i=1}^{n_s} e^{-H(\mathbf{g}_i^s)} \log\left[D\left(T\left(\mathbf{h}_i^s\right)\right)\right] + \frac{\lambda}{n_t}\sum_{j=1}^{n_t} e^{-H\left(\mathbf{g}_j^t\right)} \log\left[1 - D\left(T\left(\mathbf{h}_j^t\right)\right)\right] \\ \max_{D}\ & \frac{1}{n_s}\sum_{i=1}^{n_s} e^{-H(\mathbf{g}_i^s)} \log\left[D\left(T\left(\mathbf{h}_i^s\right)\right)\right] + \frac{1}{n_t}\sum_{j=1}^{n_t} e^{-H\left(\mathbf{g}_j^t\right)} \log\left[1 - D\left(T\left(\mathbf{h}_j^t\right)\right)\right], \end{aligned} \tag{11}$$

where λ is a hyper-parameter between source classifier and conditional domain discriminator, and note that $\mathbf{h} = (\mathbf{f}, \mathbf{g})$ is the joint variable of domain-specific feature representation $\mathbf{f}$ and classifier prediction $\mathbf{g}$ for adversarial adaptation. As a rule of thumb, we can safely set $\mathbf{f}$ as the last feature layer representation and $\mathbf{g}$ as the classifier layer prediction. In cases where lower-layer features are not transferable as in pixel-level adaptation tasks [25, 22], we can change $\mathbf{f}$ to lower-layer representations.

Generalization Error Bound We provide an analysis of our method taking similar formalism of the domain adaptation theory [5]. We first consider fixed source and target over the representation space $\mathbf{f} = F(\mathbf{x})$, and a family of source classifiers $G \in \mathcal{H}$ [13]. Denote by $\epsilon_P(G) = \mathbb{E}_{(\mathbf{f},\mathbf{y})\sim P}[G(\mathbf{f}) \neq \mathbf{y}]$ the risk of a hypothesis $G \in \mathcal{H}$ w.r.t. distribution P, and $\epsilon_P(G_1, G_2) = \mathbb{E}_{(\mathbf{f},\mathbf{y})\sim P}[G_1(\mathbf{f}) \neq G_2(\mathbf{f})]$ the disagreement between hypotheses $G_1, G_2 \in \mathcal{H}$. Let $G^* = \arg\min_G \epsilon_P(G) + \epsilon_Q(G)$ be the ideal hypothesis that explicitly embodies the notion of adaptability. The probabilistic bound [5] of the target risk $\epsilon_Q(G)$ of hypothesis G is given by the source risk $\epsilon_P(G)$ plus the distribution discrepancy:

$$\epsilon_Q(G) \leqslant \epsilon_P(G) + [\epsilon_P(G^*) + \epsilon_Q(G^*)] + |\epsilon_P(G, G^*) - \epsilon_Q(G, G^*)|. \tag{12}$$

The goal of domain adaptation is to reduce the distribution discrepancy $|\epsilon_P(G, G^*) - \epsilon_Q(G, G^*)|$.

By definition, $\epsilon_P(G, G^*) = \mathbb{E}_{(\mathbf{f},\mathbf{y})\sim P}[G(\mathbf{f}) \neq G^*(\mathbf{f})] = \mathbb{E}_{(\mathbf{f},\mathbf{g})\sim P_G}[\mathbf{g} \neq G^*(\mathbf{f})] = \epsilon_{P_G}(G^*)$, and similarly, $\epsilon_Q(G, G^*) = \epsilon_{Q_G}(G^*)$. Note that, $P_G = (\mathbf{f}, G(\mathbf{f}))_{\mathbf{f}\sim P(\mathbf{f})}$ and $Q_G = (\mathbf{f}, G(\mathbf{f}))_{\mathbf{f}\sim Q(\mathbf{f})}$ are the proxies of the joint distributions $P(\mathbf{f}, \mathbf{y})$ and $Q(\mathbf{f}, \mathbf{y})$, respectively [10]. Based on the proxies, $|\epsilon_P(G, G^*) - \epsilon_Q(G, G^*)| = |\epsilon_{P_G}(G^*) - \epsilon_{Q_G}(G^*)|$. Define a (loss) difference hypothesis space $\Delta \triangleq \{\delta = |\mathbf{g} - G^*(\mathbf{f})| \,|G^* \in \mathcal{H}\}$ over the joint variable $(\mathbf{f}, \mathbf{g})$, where $\delta : (\mathbf{f}, \mathbf{g}) \mapsto \{0, 1\}$ outputs the loss of $G^* \in \mathcal{H}$. Based on the above difference hypothesis space Δ, we define the Δ-distance as

$$\begin{aligned} d_\Delta(P_G, Q_G) &\triangleq \sup_{\delta\in\Delta} \left|\mathbb{E}_{(\mathbf{f},\mathbf{g})\sim P_G}[\delta(\mathbf{f}, \mathbf{g}) \neq 0] - \mathbb{E}_{(\mathbf{f},\mathbf{g})\sim Q_G}[\delta(\mathbf{f}, \mathbf{g}) \neq 0]\right| \\ &= \sup_{G^*\in\mathcal{H}} \left|\mathbb{E}_{(\mathbf{f},\mathbf{g})\sim P_G}[|\mathbf{g} - G^*(\mathbf{f})| \neq 0] - \mathbb{E}_{(\mathbf{f},\mathbf{g})\sim Q_G}[|\mathbf{g} - G^*(\mathbf{f})| \neq 0]\right| \\ &\geqslant \left|\mathbb{E}_{(\mathbf{f},\mathbf{g})\sim P_G}[\mathbf{g} \neq G^*(\mathbf{f})] - \mathbb{E}_{(\mathbf{f},\mathbf{g})\sim Q_G}[\mathbf{g} \neq G^*(\mathbf{f})]\right| = |\epsilon_{P_G}(G^*) - \epsilon_{Q_G}(G^*)|. \end{aligned} \tag{13}$$

Hence, the domain discrepancy $|\epsilon_P(G, G^*) - \epsilon_Q(G, G^*)|$ can be upper-bounded by the Δ-distance.

Since the difference hypothesis space Δ is a continuous function class, assume the family of domain discriminators $\mathcal{H}_D$ is rich enough to contain Δ, $\Delta \subset \mathcal{H}_D$. Such an assumption is not unrealistic as we have the freedom to choose $\mathcal{H}_D$, for example, a multilayer perceptrons that can fit any functions. Given the assumptions hold, we show that training domain discriminator D is related to $d_\Delta(P_G, Q_G)$:

$$\begin{aligned} d_\Delta(P_G, Q_G) &\leqslant \sup_{D\in\mathcal{H}_D} \left|\mathbb{E}_{(\mathbf{f},\mathbf{g})\sim P_G}[D(\mathbf{f}, \mathbf{g}) \neq 0] - \mathbb{E}_{(\mathbf{f},\mathbf{g})\sim Q_G}[D(\mathbf{f}, \mathbf{g}) \neq 0]\right| \\ &\leqslant \sup_{D\in\mathcal{H}_D} \left|\mathbb{E}_{(\mathbf{f},\mathbf{g})\sim P_G}[D(\mathbf{f}, \mathbf{g}) = 1] + \mathbb{E}_{(\mathbf{f},\mathbf{g})\sim Q_G}[D(\mathbf{f}, \mathbf{g}) = 0]\right|. \end{aligned} \tag{14}$$

This is maximized by the optimal discriminator D in CDANs, giving the upper bound of $d_\Delta(P_G, Q_G)$. Simultaneously, we learn representation $\mathbf{f}$ to minimize $d_\Delta(P_G, Q_G)$, yielding better approximation of $\epsilon_Q(G)$ by $\epsilon_P(G)$. As verified above, the proposed CDAN models formally bound the target risk.

4 Experiments

We evaluate the proposed conditional domain adversarial networks with many state-of-the-art transfer learning and deep learning methods. Codes and datasets will be available at `github.com/thuml`.

4.1 Setup

Office-31 [42] is the most widely used dataset for visual domain adaptation, with 4,652 images and 31 categories collected from three distinct domains: *Amazon* (**A**), *Webcam* (**W**) and *DSLR* (**D**). We evaluate all methods on six transfer tasks **A** $\rightarrow$ **W**, **D** $\rightarrow$ **W**, **W** $\rightarrow$ **D**, **A** $\rightarrow$ **D**, **D** $\rightarrow$ **A**, and **W** $\rightarrow$ **A**.

ImageCLEF-DA[1] is a dataset organized by selecting the 12 common classes shared by three public datasets (domains): *Caltech-256* (**C**), *ImageNet ILSVRC 2012* (**I**), and *Pascal VOC 2012* (**P**). There are 50 images in each category and 600 images in each domain, while *Office-31* has different domain sizes. We permute domains and build 6 transfer tasks: **I** $\rightarrow$ **P**, **P** $\rightarrow$ **I**, **I** $\rightarrow$ **C**, **C** $\rightarrow$ **I**, **C** $\rightarrow$ **P**, **P** $\rightarrow$ **C**.

Office-Home [54] is a better organized but more difficult dataset than *Office-31*, which consists of 15,500 images in 65 object classes in office and home settings, forming four extremely dissimilar domains: Artistic images (**Ar**), Clip Art (**Cl**), Product images (**Pr**), and Real-World images (**Rw**).

Digits We investigate three digits datasets: **MNIST**, **USPS**, and Street View House Numbers (**SVHN**). We adopt the evaluation protocol of CyCADA [22] with three transfer tasks: USPS to MNIST (**U** $\rightarrow$ **M**), MNIST to USPS (**M** $\rightarrow$ **U**), and SVHN to MNIST (**S** $\rightarrow$ **M**). We train our model using the training sets: MNIST (60,000), USPS (7,291), standard SVHN train (73,257). Evaluation is reported on the standard test sets: MNIST (10,000), USPS (2,007) (the numbers of images in the parentheses).

[1] `http://imageclef.org/2014/adaptation`

VisDA-2017[2] is a challenging simulation-to-real dataset, with two very distinct domains: **Synthetic**, renderings of 3D models from different angles and with different lightning conditions; **Real**, natural images. It contains over 280K images across 12 classes in the training, validation and test domains.

We compare Conditional Domain Adversarial Network (**CDAN**) with state-of-art domain adaptation methods: Deep Adaptation Network (**DAN**) [29], Residual Transfer Network (**RTN**) [31], Domain Adversarial Neural Network (**DANN**) [13], Adversarial Discriminative Domain Adaptation (**ADDA**) [51], Joint Adaptation Network (**JAN**) [30], Unsupervised Image-to-Image Translation (**UNIT**) [28], Generate to Adapt (**GTA**) [43], Cycle-Consistent Adversarial Domain Adaptation (**CyCADA**) [22].

We follow standard protocols for unsupervised domain adaptation [12, 30]. We use all labeled source examples and all unlabeled target examples for all datasets. We compare the average classification accuracy of each method on three random experiments, and report the standard error by all experiments of the same transfer task. We conduct the importance-weighted cross-validation [48] for all baseline methods and for our CDAN models to select hyper-parameter λ. As our CDAN models perform stably under different parameter configurations, we keep fixing $\lambda = 1$ throughout all experiments. For MMD-based methods (TCA, DAN, RTN, and JAN), we use the Gaussian kernel with bandwidth set to the median pairwise squared distances on the training data [29]. We examine the influence of deep architectures by exploring **AlexNet** [27] and **ResNet-50** [20] as base architectures, respectively.

We implement all AlexNet-based methods by **Caffe** and all ResNet-based methods by **PyTorch**. We fine-tune from the AlexNet and ResNet models pre-trained on the ImageNet dataset [41]. We fine-tune all lower layers and train the classifier layer through back-propagation, where the classifier is trained from scratch with learning rate 10 times that of the lower layers. We adopt mini-batch SGD with momentum of 0.9 and the learning rate decay strategy of DANN [13]: the learning rate is adjusted by $\eta_p = \frac{\eta_0}{(1+\alpha p)^\beta}$, where p is the training progress changing from 0 to 1, and $\eta_0 = 0.01, \alpha = 10$, $\beta = 0.75$ are optimized by the importance-weighted cross-validation [48]. We adopt a progressive training strategy for the discriminator, increasing λ from 0 to 1 by multiplying to $\frac{1-\exp(-\delta p)}{1+\exp(-\delta p)}$, $\delta = 10$.

Table 1: Accuracy (%) on *Office-31* for unsupervised domain adaptation (AlexNet and ResNet)

Method	A → W	D → W	W → D	A → D	D → A	W → A	Avg
AlexNet [27]	61.6±0.5	95.4±0.3	99.0±0.2	63.8±0.5	51.1±0.6	49.8±0.4	70.1
DAN [29]	68.5±0.5	96.0±0.3	99.0±0.3	67.0±0.4	54.0±0.5	53.1±0.5	72.9
RTN [31]	73.3±0.3	96.8±0.2	99.6±0.1	71.0±0.2	50.5±0.3	51.0±0.1	73.7
DANN [13]	73.0±0.5	96.4±0.3	99.2±0.3	72.3±0.3	53.4±0.4	51.2±0.5	74.3
ADDA [51]	73.5±0.6	96.2±0.4	98.8±0.4	71.6±0.4	54.6±0.5	53.5±0.6	74.7
JAN [30]	74.9±0.3	96.6±0.2	99.5±0.2	71.8±0.2	**58.3**±0.3	55.0±0.4	76.0
CDAN-RM	77.9±0.3	96.9±0.2	**100.0**±.0	75.1±0.2	54.5±0.3	**57.5**±0.4	77.0
CDAN-M	**78.3**±0.2	**97.2**±0.1	**100.0**±.0	**76.3**±0.1	57.3±0.2	57.3±0.3	**77.7**
ResNet-50 [20]	68.4±0.2	96.7±0.1	99.3±0.1	68.9±0.2	62.5±0.3	60.7±0.3	76.1
DAN [29]	80.5±0.4	97.1±0.2	99.6±0.1	78.6±0.2	63.6±0.3	62.8±0.2	80.4
RTN [31]	84.5±0.2	96.8±0.1	99.4±0.1	77.5±0.3	66.2±0.2	64.8±0.3	81.6
DANN [13]	82.0±0.4	96.9±0.2	99.1±0.1	79.7±0.4	68.2±0.4	67.4±0.5	82.2
ADDA [51]	86.2±0.5	96.2±0.3	98.4±0.3	77.8±0.3	69.5±0.4	68.9±0.5	82.9
JAN [30]	85.4±0.3	97.4±0.2	99.8±0.2	84.7±0.3	68.6±0.3	70.0±0.4	84.3
GTA [43]	89.5±0.5	97.9±0.3	99.8±0.4	87.7±0.5	**72.8**±0.3	**71.4**±0.4	86.5
CDAN-RM	93.0±0.2	98.4±0.2	**100.0**±.0	89.2±0.3	70.2±0.4	67.4±0.4	86.4
CDAN-M	**93.1**±0.1	**98.6**±0.1	**100.0**±.0	**92.9**±0.2	71.0±0.3	69.3±0.3	**87.5**

4.2 Results

The results on *Office-31* based on AlexNet and ResNet are reported in Table 1, with results of baselines directly reported from their original papers wherever available. The CDAN models significantly outperform all comparison methods on most transfer tasks, where CDAN-M is the top-performing variant and CDAN-RM performs slightly worse. It is desirable that CDAN promotes the classification accuracies substantially on hard transfer tasks, e.g. $\mathbf{A} \rightarrow \mathbf{W}$ and $\mathbf{A} \rightarrow \mathbf{D}$, where the source and target domains are substantially different [42]. Note that, CDAN even outperforms generative pixel-level domain adaptation method GTA, which has a very complex design in both architecture and objectives.

The results on the *ImageCLEF-DA* dataset are reported in Table 2. Our CDAN models outperform the comparison methods on most transfer tasks, but with smaller rooms of improvement. This is

[2] http://ai.bu.edu/visda-2017/

Table 2: Accuracy (%) on *ImageCLEF-DA* for unsupervised domain adaptation (AlexNet and ResNet)

Method	I → P	P → I	I → C	C → I	C → P	P → C	Avg
AlexNet [27]	66.2±0.2	70.0±0.2	84.3±0.2	71.3±0.4	59.3±0.5	84.5±0.3	73.9
DAN [29]	67.3±0.2	80.5±0.3	87.7±0.3	76.0±0.3	61.6±0.3	88.4±0.2	76.9
DANN [13]	66.5±0.6	81.8±0.3	89.0±0.4	79.8±0.6	63.5±0.5	88.7±0.3	78.2
JAN [30]	67.2±0.5	82.8±0.4	91.3±0.5	80.0±0.5	63.5±0.4	91.0±0.4	79.3
CDAN-RM	67±0.4	**84.8**±0.2	**92.4**±0.3	81.3±0.3	**64.7**±0.3	**91.6**±0.4	**80.3**
CDAN-M	**67.7**±0.3	83.3±0.1	91.8±0.2	**81.5**±0.2	63.0±0.2	91.5±0.3	79.8
ResNet-50 [20]	74.8±0.3	83.9±0.1	91.5±0.3	78.0±0.2	65.5±0.3	91.2±0.3	80.7
DAN [29]	74.5±0.4	82.2±0.2	92.8±0.2	86.3±0.4	69.2±0.4	89.8±0.4	82.5
DANN [13]	75.0±0.6	86.0±0.3	96.2±0.4	87.0±0.5	74.3±0.5	91.5±0.6	85.0
JAN [30]	76.8±0.4	88.0±0.2	94.7±0.2	89.5±0.3	74.2±0.3	91.7±0.3	85.8
CDAN-RM	77.2±0.3	88.3±0.3	**98.3**±0.4	90.7±0.4	76.7±0.3	**94.0**±0.4	87.5
CDAN-M	**78.3**±0.3	**91.2**±0.2	96.7±0.3	**91.2**±0.3	**77.2**±0.2	93.7±0.3	**88.1**

Table 3: Accuracy (%) on *Office-Home* for unsupervised domain adaptation (AlexNet and ResNet)

Method	Ar→Cl	Ar→Pr	Ar→Rw	Cl→Ar	Cl→Pr	Cl→Rw	Pr→Ar	Pr→Cl	Pr→Rw	Rw→Ar	Rw→Cl	Rw→Pr	Avg
AlexNet [27]	26.4	32.6	41.3	22.1	41.7	42.1	20.5	20.3	51.1	31.0	27.9	54.9	34.3
DAN [29]	31.7	43.2	55.1	33.8	48.6	50.8	30.1	35.1	57.7	44.6	39.3	63.7	44.5
DANN [13]	36.4	45.2	54.7	35.2	51.8	55.1	31.6	39.7	59.3	45.7	46.4	65.9	47.3
JAN [30]	35.5	46.1	57.7	36.4	53.3	54.5	33.4	40.3	60.1	45.9	47.4	67.9	48.2
CDAN-RM	36.2	47.3	58.6	37.3	54.4	**58.3**	33.2	**43.9**	62.1	48.2	48.1	70.7	49.9
CDAN-M	**38.1**	**50.3**	**60.3**	**39.7**	**56.4**	57.8	**35.5**	43.1	**63.2**	**48.4**	**48.5**	**71.1**	**51.0**
ResNet-50 [20]	34.9	50.0	58.0	37.4	41.9	46.2	38.5	31.2	60.4	53.9	41.2	59.9	46.1
DAN [29]	43.6	57.0	67.9	45.8	56.5	60.4	44.0	43.6	67.7	63.1	51.5	74.3	56.3
DANN [13]	45.6	59.3	70.1	47.0	58.5	60.9	46.1	43.7	68.5	63.2	51.8	76.8	57.6
JAN [30]	45.9	61.2	68.9	50.4	59.7	61.0	45.8	43.4	70.3	63.9	52.4	76.8	58.3
CDAN-RM	49.2	64.8	72.9	53.8	62.4	62.9	49.8	48.8	71.5	65.8	56.4	79.2	61.5
CDAN-M	**50.6**	**65.9**	**73.4**	**55.7**	**62.7**	**64.2**	**51.8**	**49.1**	**74.5**	**68.2**	**56.9**	**80.7**	**62.8**

reasonable since the three domains in *ImageCLEF-DA* are of equal size and balanced in each category, and are visually more similar than *Office-31*, making the former dataset easier for domain adaptation.

The results on *Office-Home* are reported in Table 3. Our CDAN models substantially outperform the comparison methods on most transfer tasks, and with larger rooms of improvement. An interpretation is that the four domains in *Office-Home* are with more categories, are visually more dissimilar with each other, and are difficult in each domain with much lower in-domain classification accuracy [54]. Since domain alignment is category agnostic in previous work, it is possible that the aligned domains are not classification friendly in the presence of large number of categories. It is desirable that CDAN yields larger improvements on such difficult domain adaptation tasks, which highlights the power of adversarial domain adaptation by exploiting complex multimodal structures in classifier predictions.

Strong results are also achieved on the digits datasets and synthetic to real datasets as reported in Table 4. Note that the generative pixel-level adaptation methods UNIT, CyCADA, and GTA are specifically tailored to the digits and synthetic to real adaptation tasks. This explains why the previous feature-level adaptation method JAN performs much worse. To our knowledge, CDAN is the only approach that works reasonably well on all five datasets, and remains a simple discriminative model.

Table 4: Accuracy (%) on *Digits* and *VisDA-2017* for unsupervised domain adaptation (ResNet)

Method	M → U	U → M	S → M	Avg	Method	Synthetic → Real
UNIT [28]	96.0	93.6	**90.5**	93.4	JAN [30]	61.6
CyCADA [22]	95.6	96.5	90.4	94.2	GTA [43]	69.5
CDAN-M	**96.5**	**97.1**	89.2	**94.3**	**CDAN-M**	**70.3**

4.3 Analysis

Ablation Study We study sampling strategies of the random matrices in Equation (6). We testify **CDAN-RM (Gaussian)** and **CDAN-RM (Uniform)** with their random matrices sampled only once from Gaussian and Uniform distributions, respectively. Table 5 shows that CDAN-RM (Uniform) performs better across the variants. We further investigate **CDAN-M (w/o Entropy)** and **CDAN-M (w/ Entropy)**. Table 5 depicts that CDAN-M (w/ Entropy) outperforms CDAN-M (w/o Entropy), validating the efficacy of the entropy conditioning strategy for exploring easy-to-transfer examples.

Conditioning Strategies Besides multilinear conditioning, we investigate **DANN-f** and **DANN-g** with domain discriminator plugged in feature layer $\mathbf{f}$ and classifier layer $\mathbf{g}$, **DANN-[f,g]** with domain discriminator imposed on the concatenation of $\mathbf{f}$ and $\mathbf{g}$. Figure 2(a) shows the accuracies on $\mathbf{A} \rightarrow \mathbf{W}$

Table 5: Accuracy (%) on *Office-31* of CDAN variants for unsupervised domain adaptation (ResNet)

Method	A → W	D → W	W → D	A → D	D → A	W → A	Avg
CDAN-RM (Gaussian)	91.8±0.1	97.4±0.1	99.7±0.1	87.4±0.2	**70.6**±0.3	**69.0**±0.3	86.0
CDAN-RM (Uniform)	**93.0**±0.2	**98.4**±0.2	**100.0**±.0	**89.2**±0.3	70.2±0.4	67.4±0.4	**86.4**
CDAN-M (w/o Entropy)	91.7±0.2	98.3±0.1	**100.0**±.0	92.5±0.2	70.0±0.2	67.8±0.2	86.8
CDAN-M (w/ Entropy)	**93.1**±0.1	**98.6**±0.1	**100.0**±.0	**92.9**±0.2	**71.0**±0.3	**69.3**±0.3	**87.5**

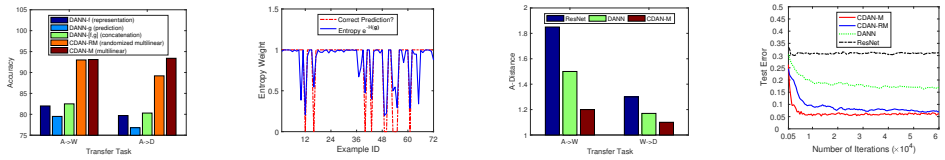

(a) Multilinear (b) Entropy (c) Discrepancy (d) Convergence

Figure 2: Empirical analysis of conditioning strategies, distribution discrepancy, and convergence.

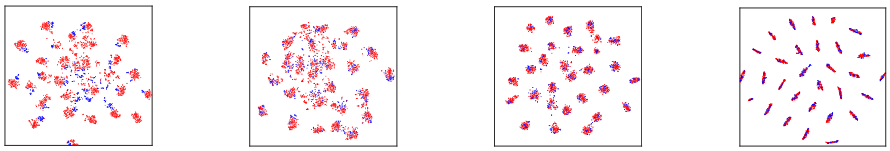

(a) ResNet (b) DANN (c) CDAN-**f** (d) CDAN-**fg**

Figure 3: T-SNE of features by (a) ResNet, (b) DANN, (c) CDAN-**f**, (d) CDAN-**fg** (red: **A**; blue: **W**).

and **A** → **D** based on ResNet-50. The concatenation strategy is not successful, as it cannot capture the cross-covariance between features and classes, which are crucial to domain adaptation [10]. Figure 2(b) shows that the entropy weight $e^{-H(\mathbf{g})}$ corresponds well with the prediction correctness: entropy weight ≈ 1 when the prediction is correct, and much smaller than 1 when prediction is incorrect (uncertain). This reveals the power of the entropy conditioning to guarantee example transferability.

Distribution Discrepancy The $\mathcal{A}$-distance is widely used as a measure of distribution discrepancy [5, 33], defined as $d_{\mathcal{A}} = 2\,(1 - 2\epsilon)$, where ϵ is the test error of a classifier trained to discriminate source and target. Figure 2(c) shows $d_{\mathcal{A}}$ on tasks **A** → **W**, **W** → **D** with features of ResNet, DANN, and CDAN-M. We observe that $d_{\mathcal{A}}$ on CDAN-M features is smaller than $d_{\mathcal{A}}$ on ResNet and DANN features, implying that CDAN-M features can reduce the domain gap more effectively. As domains **W** and **D** are similar, $d_{\mathcal{A}}$ of task **W** → **D** is smaller than that of **A** → **W**, implying higher accuracies.

Convergence We testify the convergence of ResNet, DANN, and CDANs, with the test errors on task **A** → **W** shown in Figure 2(d). CDAN enjoys faster convergence than DANN, while CDAN-M converges faster than CDAN-RM. Note that CDAN-M deals with high-dimensional multilinear map, thus each iteration costs slightly more than CDAN-RM, while CDAN-RM has similar cost as DANN.

Visualization We visualize by t-SNE [32] in Figures 3(a)–3(d) the activations of task **A** → **W** (31 classes) by ResNet, DANN, CDAN-f, and CDAN-fg. The source and target are not aligned well with ResNet, better aligned with DANN but categories are not discriminated well. They are aligned better and categories are discriminated better by CDAN-f, while CDAN-fg is evidently better than CDAN-f. This shows the benefit of conditioning domain adversarial adaptation on discriminative predictions.

5 Conclusion

This paper presented conditional domain adversarial network (CDAN), a novel approach to domain adaptation with multimodal distributions. Unlike previous adversarial adaptation methods that solely match the feature representation across domains which is prone to under-matching, the proposed approach further conditions the adversarial domain adaptation on discriminative information to enable alignment of multimodal distributions. Experiments validated the efficacy of the proposed approach.

Acknowledgments

We thank Yuchen Zhang at Tsinghua University for insightful discussions. This work was supported by the National Key R&D Program of China (No. 2016YFB1000701), Natural Science Foundation of China (61772299, 61502265, 71690231) and DARPA Program on Lifelong Learning Machines.

References

[1] M. Arjovsky and L. Bottou. Towards principled methods for training generative adversarial networks. In *International Conference on Learning Representations (ICLR)*, 2017.

[2] M. Arjovsky, S. Chintala, and L. Bottou. Wasserstein gan. In *International Conference on Machine Learning (ICML)*, 2017.

[3] S. Arora, R. Ge, Y. Liang, T. Ma, and Y. Zhang. Generalization and equilibrium in generative adversarial nets (gans). In *International Conference on Machine Learning (ICML)*, 2017.

[4] S. Arora and Y. Zhang. Do gans actually learn the distribution? an empirical study. *arXiv preprint arXiv:1706.08224*, 2017.

[5] S. Ben-David, J. Blitzer, K. Crammer, A. Kulesza, F. Pereira, and J. W. Vaughan. A theory of learning from different domains. *Machine Learning*, 79(1-2):151–175, 2010.

[6] Y. Bengio, A. Courville, and P. Vincent. Representation learning: A review and new perspectives. *IEEE Transactions on Pattern Analysis and Machine Intelligence (TPAMI)*, 35(8):1798–1828, 2013.

[7] T. Che, Y. Li, A. P. Jacob, Y. Bengio, and W. Li. Mode regularized generative adversarial networks. *International Conference on Learning Representations (ICLR)*, 2017.

[8] Y. Chen, W. Chen, Y. Chen, B. Tsai, Y. F. Wang, and M. Sun. No more discrimination: Cross city adaptation of road scene segmenters. In *The IEEE International Conference on Computer Vision (ICCV)*, pages 2011–2020, 2017.

[9] R. Collobert, J. Weston, L. Bottou, M. Karlen, K. Kavukcuoglu, and P. Kuksa. Natural language processing (almost) from scratch. *Journal of Machine Learning Research (JMLR)*, 12:2493–2537, 2011.

[10] N. Courty, R. Flamary, A. Habrard, and A. Rakotomamonjy. Joint distribution optimal transportation for domain adaptation. In *Advances in Neural Information Processing Systems 30*, pages 3730–3739. 2017.

[11] J. Donahue, Y. Jia, O. Vinyals, J. Hoffman, N. Zhang, E. Tzeng, and T. Darrell. Decaf: A deep convolutional activation feature for generic visual recognition. In *International Conference on Machine Learning (ICML)*, 2014.

[12] Y. Ganin and V. Lempitsky. Unsupervised domain adaptation by backpropagation. In *International Conference on Machine Learning (ICML)*, 2015.

[13] Y. Ganin, E. Ustinova, H. Ajakan, P. Germain, H. Larochelle, F. Laviolette, M. Marchand, and V. Lempitsky. Domain-adversarial training of neural networks. *The Journal of Machine Learning Research (JMLR)*, 17(1):2096–2030, 2016.

[14] X. Glorot, A. Bordes, and Y. Bengio. Domain adaptation for large-scale sentiment classification: A deep learning approach. In *International Conference on Machine Learning (ICML)*, 2011.

[15] B. Gong, K. Grauman, and F. Sha. Connecting the dots with landmarks: Discriminatively learning domain-invariant features for unsupervised domain adaptation. In *International Conference on Machine Learning (ICML)*, 2013.

[16] B. Gong, Y. Shi, F. Sha, and K. Grauman. Geodesic flow kernel for unsupervised domain adaptation. In *IEEE Conference on Computer Vision and Pattern Recognition (CVPR)*, 2012.

[17] I. Goodfellow, J. Pouget-Abadie, M. Mirza, B. Xu, D. Warde-Farley, S. Ozair, A. Courville, and Y. Bengio. Generative adversarial nets. In *Advances in Neural Information Processing Systems (NIPS)*, 2014.

[18] R. Gopalan, R. Li, and R. Chellappa. Domain adaptation for object recognition: An unsupervised approach. In *IEEE International Conference on Computer Vision (ICCV)*, 2011.

[19] Y. Grandvalet and Y. Bengio. Semi-supervised learning by entropy minimization. In *Advances in Neural Information Processing Systems*, 2005.

[20] K. He, X. Zhang, S. Ren, and J. Sun. Deep residual learning for image recognition. In *IEEE Conference on Computer Vision and Pattern Recognition (CVPR)*, 2016.

[21] J. Hoffman, S. Guadarrama, E. Tzeng, R. Hu, J. Donahue, R. Girshick, T. Darrell, and K. Saenko. LSDA: Large scale detection through adaptation. In *Advances in Neural Information Processing Systems*, 2014.

[22] J. Hoffman, E. Tzeng, T. Park, J.-Y. Zhu, P. Isola, K. Saenko, A. Efros, and T. Darrell. CyCADA: Cycle-consistent adversarial domain adaptation. In *Proceedings of the 35th International Conference on Machine Learning*, pages 1989–1998, 2018.

[23] J. Hoffman, D. Wang, F. Yu, and T. Darrell. Fcns in the wild: Pixel-level adversarial and constraint-based adaptation. *CoRR*, abs/1612.02649, 2016.

[24] J. Huang, A. J. Smola, A. Gretton, K. M. Borgwardt, and B. Schölkopf. Correcting sample selection bias by unlabeled data. In *Advances in Neural Information Processing Systems (NIPS)*, 2006.

[25] P. Isola, J.-Y. Zhu, T. Zhou, and A. A. Efros. Image-to-image translation with conditional adversarial networks. In *IEEE Conference on Computer Vision and Pattern Recognition (CVPR)*, 2017.

[26] P. Kar and H. Karnick. Random feature maps for dot product kernels. In *International Conference on Artificial Intelligence and Statistics (AISTATS)*, volume 22, pages 583–591, 2012.

[27] A. Krizhevsky, I. Sutskever, and G. E. Hinton. Imagenet classification with deep convolutional neural networks. In *Advances in Neural Information Processing Systems (NIPS)*, 2012.

[28] M.-Y. Liu, T. Breuel, and J. Kautz. Unsupervised image-to-image translation networks. In *Advances in Neural Information Processing Systems 30*, pages 700–708. 2017.

[29] M. Long, Y. Cao, J. Wang, and M. I. Jordan. Learning transferable features with deep adaptation networks. In *International Conference on Machine Learning (ICML)*, 2015.

[30] M. Long, J. Wang, and M. I. Jordan. Deep transfer learning with joint adaptation networks. In *International Conference on Machine Learning (ICML)*, 2017.

[31] M. Long, H. Zhu, J. Wang, and M. I. Jordan. Unsupervised domain adaptation with residual transfer networks. In *Advances in Neural Information Processing Systems (NIPS)*, pages 136–144, 2016.

[32] L. v. d. Maaten and G. Hinton. Visualizing data using t-sne. *Journal of Machine Learning Research (JMLR)*, 9(Nov):2579–2605, 2008.

[33] Y. Mansour, M. Mohri, and A. Rostamizadeh. Domain adaptation: Learning bounds and algorithms. In *Conference on Computational Learning Theory (COLT)*, 2009.

[34] M. Mirza and S. Osindero. Conditional generative adversarial nets. *arXiv preprint arXiv:1411.1784*, 2014.

[35] A. Odena, C. Olah, and J. Shlens. Conditional image synthesis with auxiliary classifier gans. In *International Conference on Machine Learning (ICML)*, 2017.

[36] M. Oquab, L. Bottou, I. Laptev, and J. Sivic. Learning and transferring mid-level image representations using convolutional neural networks. In *IEEE Conference on Computer Vision and Pattern Recognition (CVPR)*, 2013.

[37] S. J. Pan, I. W. Tsang, J. T. Kwok, and Q. Yang. Domain adaptation via transfer component analysis. *IEEE Transactions on Neural Networks (TNN)*, 22(2):199–210, 2011.

[38] S. J. Pan and Q. Yang. A survey on transfer learning. *IEEE Transactions on Knowledge and Data Engineering (TKDE)*, 22(10):1345–1359, 2010.

[39] J. Quionero-Candela, M. Sugiyama, A. Schwaighofer, and N. D. Lawrence. *Dataset shift in machine learning*. The MIT Press, 2009.

[40] A. Rahimi and B. Recht. Random features for large-scale kernel machines. In *Advances in neural information processing systems (NIPS)*, pages 1177–1184, 2008.

[41] O. Russakovsky, J. Deng, H. Su, J. Krause, S. Satheesh, S. Ma, Z. Huang, A. Karpathy, A. Khosla, M. Bernstein, A. C. Berg, and L. Fei-Fei. ImageNet Large Scale Visual Recognition Challenge. 2014.

[42] K. Saenko, B. Kulis, M. Fritz, and T. Darrell. Adapting visual category models to new domains. In *European Conference on Computer Vision (ECCV)*, 2010.

[43] S. Sankaranarayanan, Y. Balaji, C. D. Castillo, and R. Chellappa. Generate to adapt: Aligning domains using generative adversarial networks. In *The IEEE Conference on Computer Vision and Pattern Recognition (CVPR)*, June 2018.

[44] L. Song, B. Boots, S. M. Siddiqi, G. J. Gordon, and A. Smola. Hilbert space embeddings of hidden markov models. In *International Conference on Machine Learning (ICML)*, 2010.

[45] L. Song and B. Dai. Robust low rank kernel embeddings of multivariate distributions. In *Advances in Neural Information Processing Systems (NIPS)*, pages 3228–3236, 2013.

[46] L. Song, K. Fukumizu, and A. Gretton. Kernel embeddings of conditional distributions: A unified kernel framework for nonparametric inference in graphical models. *IEEE Signal Processing Magazine*, 30(4):98–111, 2013.

[47] L. Song, J. Huang, A. Smola, and K. Fukumizu. Hilbert space embeddings of conditional distributions with applications to dynamical systems. In *International Conference on Machine Learning (ICML)*, 2009.

[48] M. Sugiyama, M. Krauledat, and K.-R. Muller. Covariate shift adaptation by importance weighted cross validation. *Journal of Machine Learning Research (JMLR)*, 8(May):985–1005, 2007.

[49] M. Sugiyama, S. Nakajima, H. Kashima, P. V. Buenau, and M. Kawanabe. Direct importance estimation with model selection and its application to covariate shift adaptation. In *Advances in Neural Information Processing Systems (NIPS)*, 2008.

[50] Y. Tsai, W. Hung, S. Schulter, K. Sohn, M. Yang, and M. Chandraker. Learning to adapt structured output space for semantic segmentation. In *IEEE Conference on Computer Vision and Pattern Recognition (CVPR)*, 2018.

[51] E. Tzeng, J. Hoffman, K. Saenko, and T. Darrell. Adversarial discriminative domain adaptation. In *IEEE Conference on Computer Vision and Pattern Recognition (CVPR)*, 2017.

[52] E. Tzeng, J. Hoffman, N. Zhang, K. Saenko, and T. Darrell. Deep domain confusion: Maximizing for domain invariance. *CoRR*, abs/1412.3474, 2014.

[53] E. Tzeng, J. Hoffman, N. Zhang, K. Saenko, and T. Darrell. Simultaneous deep transfer across domains and tasks. In *IEEE International Conference on Computer Vision (ICCV)*, 2015.

[54] H. Venkateswara, J. Eusebio, S. Chakraborty, and S. Panchanathan. Deep hashing network for unsupervised domain adaptation. In *IEEE Conference on Computer Vision and Pattern Recognition (CVPR)*, 2017.

[55] J. Yosinski, J. Clune, Y. Bengio, and H. Lipson. How transferable are features in deep neural networks? In *Advances in Neural Information Processing Systems (NIPS)*, 2014.

[56] K. Zhang, B. Schölkopf, K. Muandet, and Z. Wang. Domain adaptation under target and conditional shift. In *International Conference on Machine Learning (ICML)*, 2013.

[57] J.-Y. Zhu, T. Park, P. Isola, and A. A. Efros. Unpaired image-to-image translation using cycle-consistent adversarial networks. In *The IEEE International Conference on Computer Vision (ICCV)*, Oct 2017.